Spray and Combustion Characterizations of Acetone-Butanol-Ethanol (ABE) blend in High-Pressure and High-Temperature Conditions

Ob Nilaphai[*1], Hugo Ajrouche[1], Camille Hespel[1], Bruno Moreau[1], Somchai Chanchaona[2], Fabrice Foucher[1], Christine Mounaim-Rousselle[1]

[1]PRISME, Université d'Orléans, France

[2]CERL, King Mongkut's University of Technology Thonburi, Thailand

*Corresponding author: ob.nilaphai@etu.univ-orleans.fr

Abstract

The intermediate fermentation mixture of butanol production, Acetone, Butanol and Ethanol (ABE), is increasingly considered as a new alternative fuel in CI engines due to its physical and chemical properties, which are similar to those of butanol, and its advantages of no additional cost or energy consumption due to butanol separation. In a previous study, the High-Pressure and High-Temperature (HPHT) chamber, called 'New One Shot Engine" (NOSE), was used to investigate macroscopic spray-combustion parameters by validating Spray-A conditions of the Engine Combustion Network. The present study concerns the spray-combustion characteristics of the ABE mixture (volume ratio 3:6:1), blended with n-dodecane at a volumetric ratio of 20% (ABE20), compared to n-dodecane as reference fuel. The macroscopic spray and combustion parameters were investigated, for non-reactive conditions, in pure Nitrogen and for reactive conditions, in 15% oxygen, at ambient pressure (60 bar), ambient density (22.8 kg/m^3) and different ambient temperatures (800 K, 850 K and 900 K). The liquid and vapor spray penetrations were investigated by the Diffused Back Illumination (DBI) and Schlieren techniques in non-reactive conditions. In reactive conditions, the lift-off length was measured by OH* chemiluminescence images at 310 nm. The Schlieren technique was also used to verify the choice of detection criterion. The ignition delay results of the two fuels were compared. It was found that the behavior of the two fuels as a function of temperature was similar even if the liquid length of ABE20 was shorter than that of n-dodecane at all ambient temperatures. On the other hand, no real difference in vapor spray penetration between the two fuels was observed. The vaporization properties and the lower auto-ignition ability of ABE20 led to longer ignition delays and lift-off length.

Keywords

Spray and Combustion Characterizations, Acetone-Butanol-Ethanol (ABE), High-Pressure and High-Temperature Conditions.

Introduction

Due to the increase in energy demand and the depletion of oil resources during the last few decades, butanol has become an alternative fuel, considered in the transportation sector as a sustainable energy and also a means to reduce greenhouse gases compared to conventional fuel [1], as it can be produced from renewable bioresources in the form of agricultural biomass and waste [2]. Moreover, butanol induces lower fuel consumption as its energy content is higher than ethanol, up to 30%, and its lower water solubility decreases the tendency to microbial-induced corrosion in fuel storage and pipelines during transportation [1]. The higher cetane number (CN) of butanol (CN = 25) compared to ethanol (CN = 8) leads to easier ignition in compression ignition (CI) engines [3]. It is suitable for diesel injection systems thanks to its high level of viscosity like diesel fuel and no water content, unlike ethanol. Finally, researchers have considered butanol as one means to reduce CO, HC, NOx, and Soot emissions [4] and also to improve combustion efficiency especially in advanced combustion modes [5].

Bio-butanol can be produced from agricultural crops and lignocellulosic biomass by using Clostridium bacteria, Clostridium beijerinckii or Clostridium acetobutylicum, to ferment lignocellulosic hydrolysate sugars to produce a mixture of Acetone, Butanol and Ethanol (ABE) in a volume ratio of 3:6:1 [6], [7], after which it is distilled to separate butanol from the ABE mixture. However, the intermediate fermentation product, ABE, can also be considered as a potential new alternative fuel itself for CI engines because its physical and chemical properties are similar to those of butanol [3], [7], [8]. In addition, if the ABE mixture can be used as fuel, the cost and energy consumption of the separation process of butanol from ABE would be eliminated.

The Engine Combustion Network (ECN), initiated by Sandia National Lab, is an international network for the experimental and simulation analysis of combustion phenomena for diesel and gasoline engines to provide new accurate data about diesel spray and combustion processes and thereby reach a better understanding of the physical processes involved and also of the modelling concepts and models themselves [9], [10]. To participate in this network, PRISME Laboratory University of Orleans developed a new chamber to reach the High Pressure-High Temperature (HPHT) thermodynamic conditions of current common-rail diesel engines, called 'New One Shot Engine" (NOSE), designed based on the concept of the Rapid Cycling Machine (RCYM).

In a previous study, NOSE was successfully used to investigate the macroscopic spray parameters of n-dodecane by using standard conditions and standard measurement methods in the Spray-A conditions of the Engine Combustion Network (ECN) [10]. The present study focuses on the spray – combustion parameters in the case of an ABE mixture, blended with n-dodecane in a volume ratio of 20% (ABE20) in comparison to the reference fuel, n-dodecane. The macroscopic spray parameters and combustion parameters were investigated in non-reactive conditions (pure Nitrogen) and reactive conditions (15% oxygen) at ambient pressure (near 60 bar), ambient density (22.8 kg/m^3) and different ambient temperatures (800 K, 850 K, and 900 K). The injection conditions were controlled at 1,500 bar of injection pressure, 90 ºC of injection fuel temperature, and 1.5 ms of injection duration. The results of macroscopic spray, the liquid length (LL) and vapor spray penetration (S) were investigated by the Diffused Back Illumination (DBI) and Schlieren techniques for non-reactive conditions. In reactive conditions, the Lift-off Length (LOL) was measured by OH* chemiluminescence images at 310 nm. In the last section, the results of ignition delay (ID) for the two fuels are discussed and compared. The Schlieren technique was used to verify the detection criterion to determine the ignition delay by OH* chemiluminescence.

Experimental set-up and operating conditions

NOSE is a High Pressure-High Temperature (HPHT) combustion chamber which operates based on the concept of the Rapid Cycling Machine (RCYM). It was developed to study diesel spray and combustion with the objective of sharing experimental conditions defined by the ECN [10]. The NOSE design is based on the use of a single-cylinder low-speed diesel engine with a 155 mm bore diameter and 177.8 mm stroke. The original cylinder head was replaced by a dedicated chamber, designed by extending the combustion chamber to support optical measurements. The compression ratio was set at 15:1 by modifying the shape of the piston head. There are 4 quartz windows, 25 mm thick, 25 mm wide, and 80 mm long to support several kinds of optical measurement. Further details about the chamber design, thermal characterization chamber, specification of the injection system, and data acquisition system were presented in our previous study [10].

To achieve target conditions in an adiabatic compression process, the initial conditions such as initial pressure, temperature, and injection temperature must be defined before starting operation. For example, in the non-reactive condition of 900 K, the piston was first positioned at BDC with a cooling temperature fixed at 83 °C. The chamber was heated up to 100.5 °C to achieve 90 °C inside the injector 'sac'. The chamber was filled with Pure Nitrogen (N$_2$) until 1.8 bar of initial pressure was reached. The electric motor drives the piston from BDC to TDC to compress gas inside the chamber. Around TDC, the control system generates the TTL signal to drive fuel injection during 1.5 ms and to trigger image recording. The main testing conditions are summarized in Table 1.

Table 1. The main conditions of test fuels at the Start Of Injection (SOI)

Parameters	Value
Ambient gas temperature	800, 850, 900 K
Ambient gas pressure	near 60 bar
Ambient gas density	22.8 kg/m^3
Ambient gas oxygen	0% O$_2$ for non-reactive
	15% O$_2$ for reactive
Ambient gas velocity	Near-quiescent, less than 1 m/s
Fuel injection pressure	150 MPa (1,500 bar)
Fuels	n-dodecane, and ABE20
Fuel temperature at nozzle	363 K (90°C)
Injection duration	1.5 ms

In this study, the ABE used was based on the typical volume ratio 3:6:1 [7] (30% of acetone, 60% of butanol, and 10% of ethanol with acetone (98.5%), butanol (99.5%), and ethanol (99.5%)). The ABE mixture was blended with n-dodecane, at a volumetric ratio of 20% (ABE20), as n-dodecane is a conventional surrogate of diesel fuel. The physical properties of the fuels are given in Table 2. The density and viscosity were measured by a viscosity meter (Anton Paar SVM300) and the other properties were taken from the literature [11]-[13], if available.

Table 2. Fuel properties

Properties	n-Dodecane	Acetone	Butanol	Ethanol	ABE20
Molecular formula	$C_{12}H_{26}$	C_3H_6O	C_4H_9OH	C_2H_5OH	-
Density at 15 °C (kg/m^3)	752.8	789	813.3	794.1	760.7
Viscosity at 15 °C (mm^2/s)	2.032	0.149	4.119	1.489	1.642
Cetane number [11]	74	-	17	8	-
Boiling point (K) [12]	489.3	329.1	390.6	351.3	-
Vapor pressure at 298 K (kPa) [12]	0.018	30.80	0.58	7.91	-
Latent heat of Vaporization at 298 K (kJ/kg) [12], [13]	362	518	582	904	-

Optical techniques

In this part the details of the different optical techniques and post-processing tools are explained. Table 3 summarizes the optical set-ups, for the 4 different techniques needed to characterize macroscopic spray of non-reactive and combustion parameters, following the ECN recommendations to ensure accurate experimental results.

Table 3. Summary of the optical set-ups

	Non-Reactive		Reactive		
Optical Technique	DBI	Schlieren	OH* Chemilu.	Schlieren	OH* Chemilu.
Parameters	Liquid Penetration Length (LL)	Vapor Spray Penetration (S)	Lift-Off Length (LOL)	Ignition Delay (ID)	Ignition Delay (ID)
Camera / Detector	Phantom-V1611	Phantom-V1611	Photron - APX-I2	Phantom-V1611	Newport Photomultiplier tube 70680
Sensor type	CMOS	CMOS	ICCD	CMOS	-
Light source	LED plate (white) 100x100 mm	LED (white) with 1 mm pinhole	-	LED (white) with 1 mm pinhole	-
Lens	60 mm f/2.8	-	UV 60 mm f/3.5	-	-
Mirrors	-	2 Parabolic Mirrors 34 inch	-	2 Parabolic Mirrors 34 inch	-
Pin hole	-	6 mm	-	6 mm	-
Filter	-	-	BPF 310 nm FWHM 10 nm	LPF ≤ 550 nm	BPF 307 nm FWHM 10 nm
Frame speed	49 kHz	39 kHz	2 kHz	39 kHz	-
Exposure time	3 µs	5 µs	499 µs	5 µs	-
Image size	512 x 384 pi²	1024 x 400 pi²	512 x 1024 pi²	1024 x 400 pi²	-
Magnification	12 pix/mm	12.3 pix/mm	18.2 pix/mm	12.3 pix/mm	-
Repetitions	12 tests	12 tests	12 tests	12 tests	12 tests

Diffused Back Illumination (DBI)

The liquid penetration length (LL) is an important parameter when designing and optimizing the operation of modern diesel engines. The length of liquid-phase fuel needs to be optimized to avoid fuel impinging on and collecting at the piston bowl or cylinder wall, which causes higher emissions. The liquid penetration length is defined as the maximum distance of liquid-phase from the injector tip to liquid phase fuel penetration [14], [15]. To avoid uncertainties due to the light source, the calibration and the post-processing, DBI is recommended by the ECN as the standard technique to measure LL [9], [16]. Moreover, DBI is easy to implement as it consists of only two main components: the light source and the camera, as shown in Figure 1 (left).

A white LED light plate measuring 100x100 mm² was used to illuminate the liquid phase of spray. The light intensity through the optical window and images from the test section were collected by the high speed camera (Phantom V1611), as shown in Figure 1 (left). The flame rate, exposure time, and image resolution were set at suitable values to capture high quality images (512x512 pi²) at a high frequency (49 kHz), as shown in Table 3.

For post-processing, the light intensity of background images (I_{bg}) was processed from the average of images before start of injection (SOI). The average light intensity (I_{avg}) was normalized by I_{bg}. The images during steady-state of injection, i.e. 1.1 to 1.5 ms after SOI, were averaged to avoid the transient phases due to the start and end of injection. Then the light extinction factor, τ, along the spray core was calculated from equation (1). The light extinction image is shown in Figure 1 (right-top). To avoid the effect of the beam steering phenomenon due to variation in the refraction index on the medium at the liquid spray tip, the distance where the linear fit line (red line) crosses the X-axis was determined as the liquid length (LL) of spray penetration, as shown in Figure 1 (right-bottom).

$$\tau(x, y) = -log\left(\frac{I_{avg}(x,y)}{I_{bg}(x,y)}\right) \tag{1}$$

Figure 1. Scheme of DBI set-up (left), the light extinction image (right-top), and LL determination criterion (right-bottom)

Schlieren visualization

To detect the vapor phase of the spray, the high-sensitivity Schlieren technique was used, based on the measurement of the bending of the light source though the test section, which is sensitive enough to capture the spray boundary. The pinhole or aperture Schlieren stop was used to give a bright field and dark background. The image processing and determination of S were done by using the standardized post-processing code of Sandia to reduce uncertainties and to compare and validate the values obtained. Figure 2 (left) shows an example of Schlieren images and an example of the spray boundary (red line). The vapor spray penetration length is defined at the spray front that crosses the spray axis (vertical blue line). The Schlieren set-up, presented in Figure 2 (right), is composed of a continuous white LED with a 1 mm pinhole, mirrors and collimating mirrors to reflect light through the test section in the NOSE chamber. A 6 mm pinhole was set up to record Schlieren light by the high speed camera (Phantom V1611). The image resolution was 1024x400 pixels, and the highest flame rate was set at 39 kHz, with an exposure time of 5 µs.
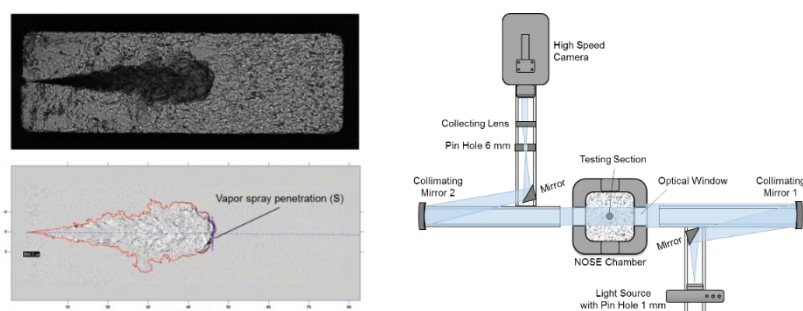

Figure 2. An example of Schlieren images (left-top) and an example of the spray boundary (left-bottom). Experimental scheme of Schlieren set-up. (right)

In reactive conditions three optical techniques were set up to measure the combustion parameters at the same time, namely a lift-off length by OH* chemiluminescence images at 310 nm, an ignition delay from high speed Schlieren images, and the OH* chemiluminescence temporal signal recorded by the photomultiplier as shown in Figure 3.
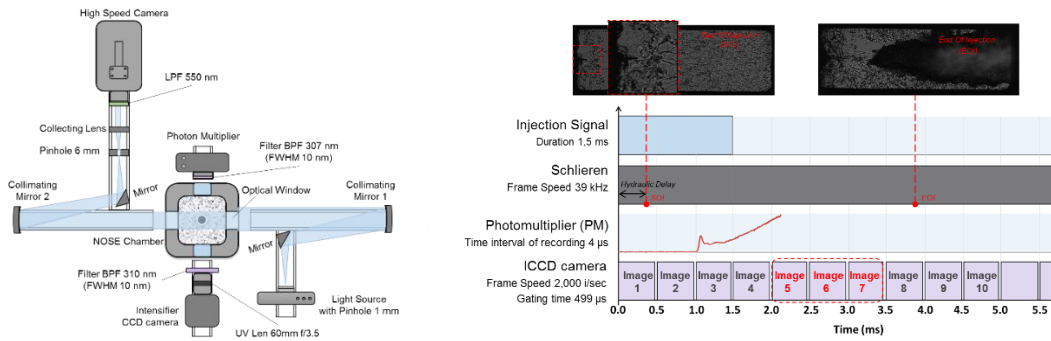
Figure 3. The optical set-ups for reactive condition (left) and synchronization signals diagram (right). The images 5, 6 and 7 (2.0 ms after SOI) of ICCD camera were used to calculate the LOL.

Lift-Off Length

Generally, Lift-Off Length is defined as the distance between the injector tip and the stabilized flame of the high temperature reaction zone [17], [18]. As is well known, at high temperature the chemiluminescence spectrum of OH* is centered at 310 nm, so OH* is a good indicator to measure the LOL. As shown in Figure 3, an ICCD Photron Fastcam APX I2 was used with a 60 mm f/3.5 UV lens and equipped with a 310 nm (FWHM10) band-pass filter (BFP). A long constant gating time of 449 µs was used to allow turbulent fluctuation in the LOL to reach an average so as to provide an image of the quasi-steady mean LOL after start of injection (SOI) [17]. 10 images were recorded and the image taken during quasi-steady state, as well as images 5, 6 and 7 (2.0 ms after SOI) were used to calculate the LOL as shown in Figure 3 (left). Figure 4 (left) shows the post-processing criterion; the intensity along the upper (red) and lower (blue) profile of the spray centerline is considered to define LOL. In this study LOL was defined as the average distance between the injector tip and the first value above 50% of the maximum intensity of each profile, following the ECN method [9]. Figure 4 (right) shows an example of the LOL of n-dodecane at 850 K.
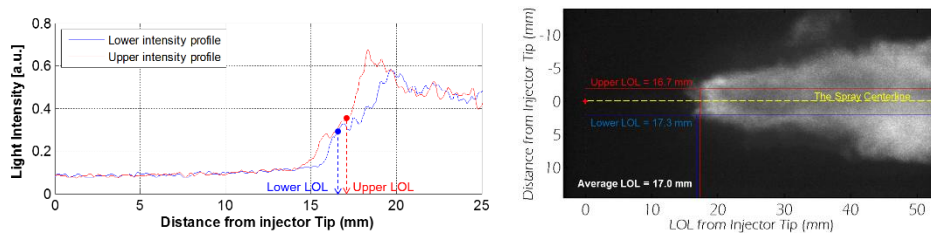

Figure 4. The light intensity along the upper and lower profile of the spray centreline and the dots represent the 50% of the maximum intensity of each profile (left) and an example of LOL result at 850 K of n-dodecane (right).

Ignition Delay

To determine the ability of fuels to auto-ignite, the ignition delays of n-dodecane and ABE20 were characterized and compared. During the combustion process, there are two states of ignition: the first state of ignition or cool flame, and the second state of ignition or hot flame [15]. The cool flame is the moment at which the first light is emitted by natural luminosity, when the parent fuel molecules are broken down and raise the temperature slightly. However, during this stage it cannot be detected by an increase in cylinder pressure but by the emission of CH radicals [15], [19]. After that the hot flame occurs, which can be characterized by OH radicals chemiluminescence in UV at 310 nm [9], [15], [18]. In this paper the ignition delay was defined as the time between the start of injection and the second stage of ignition or hot flame ignition delay. The start of injection (SOI) is an important parameter that should be clearly defined before calculating the ignition delay. It was defined here as the time between the start of injection current and the first injection image of the spray obtained by Schlieren visualization, usually called "hydraulic delay". To use the same criterion to define ignition delay with both techniques, the results shown in this work were corrected by the hydraulic delay.

The hot flame ignition delay was detected by the Schlieren technique, which was set as for the reactive condition, but a 550 nm low-pass filter was added to limit emissions due to soot radiation. Figure 5 (left) shows the Schlieren images during cool flame and hot flame events. As mentioned before, the hot flame ignition delay appears after the cool flame. The cool flame can be detected at the extinction region in the reactive Schlieren images. This can be explained by the fact that during this period the slight increase in temperature changes the refractive index of the spray to match the refractive index of the ambient gas, leading to more transparent images than the original Schlieren images [20]. Figure 5 (left) shows the series of cool flame images and post-processing images. The vapor

spray length in transparent images is shorter after post-processing when compared with non-reactive events, as shown in Figure 5 (right) from 312.9 μs to 373.1 μs. After that, the head of spray images reappear at 398.7 μs and the curve again becomes similar to that of the non-reactive events. In the next images the head of spray smoothly expands in the radial and axial directions. The red point in Figure 5 (right) marks the onset of combustion, which corresponds to the second image after the return to the normal trend. This enables the hot flame ignition delay of the different fuels to be compared.

To verify the criterion defined for Schlieren images, OH* chemiluminescence was also used to detect the hot flame ignition delay. As can be seen in Table 3, a Newport Oriel Photomultiplier tube side-on with a PMT 70705 high voltage power supply and a band-pass filter of 307 nm (FWHM 10) was used to follow OH* chemiluminescence temporally. It was set up close to the NOSE window and positioned on the opposite side to the ICCD camera, as shown in Figure 3 (left). The low light intensity signal from the combustion event was multiplied and recorded in an in-house Labview data acquisition system (DAQ) with a 4 μs recording interval. The time at the start of combustion of the hot flame is defined at the maximum of the first peak. Figure 5 (right) shows that the two techniques used to identify ignition delays are in good agreement.
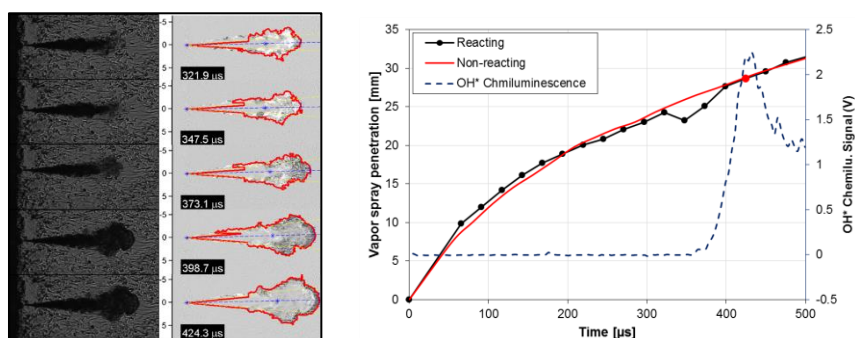

Figure 5. The series of Schlieren images and post-processed images during cool flame and hot flame events (left) and validation of the ignition delay criterion on Schlieren images by the OH* chemiluminescence collected by a Photomultiplier at 900 K on n-dodecane (right).

Result and discussion

This section presents the results of spray and combustion parameters at different ambient conditions for both fuels, n-dodecane and ABE20. All the results are averages of 12 tests; standard deviation bars are indicated.

Liquid penetration length

Figure 6 shows the results of LL for both fuels at different ambient temperatures. As expected, LL is longer at lower ambient temperature than at high temperatures, there is more energy entrainment on the liquid fuel, leading to an increase in the evaporation rate and also as the surface tension and viscosity of the fuel are lower, the atomization process is enhanced [7], [14]. The LL of ABE20 are shorter than those of n-dodecane for all ambient conditions, mainly due to the higher volatility of solution fuels in ABE20. From the physical properties shown in Table 2, the boiling point of the fuel components of ABE20 is 32.7%, 20.2%, and 28.2% lower than that of n-dodecane for acetone, butanol, and ethanol, respectively. Moreover, the vapor pressure of acetone, butanol, and ethanol is 30.8 kPa, 0.58 kPa, and 7.9 kPa, which is much higher than that of n-dodecane (0.018 kPa). This leads to a faster evaporation rate for ABE20.
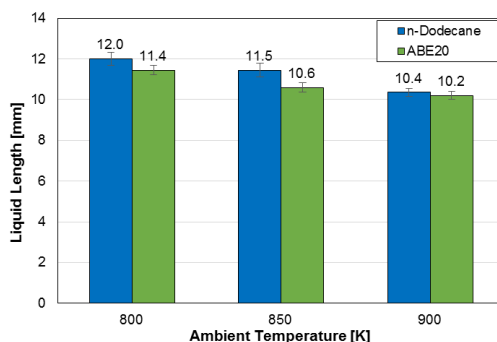

Figure 6. Liquid penetration length (LL) results for different tests.

Vapour spray penetration length

Figure 7 (left) shows the vapor spray penetration of ABE20 for different ambient temperatures. It can be observed that there is no significant difference (1% of variation in average) and this trend is also the same in n-dodecane. The vapor spray penetration depends mainly on the spray momentum which is controlled by the injection pressure (1500 bar), the fuel density and the gas density, set at 22.8 kg/m^3 whatever the ambient temperature. The effect of fuel on vapor length is presented in Figure 7 (right). The blue line represents the average S (from 3 ambient temperatures) of ABE20 and the red line the average S of n-dodecane. There is no significant difference in the trends of the two fuels (2% of variation in average).
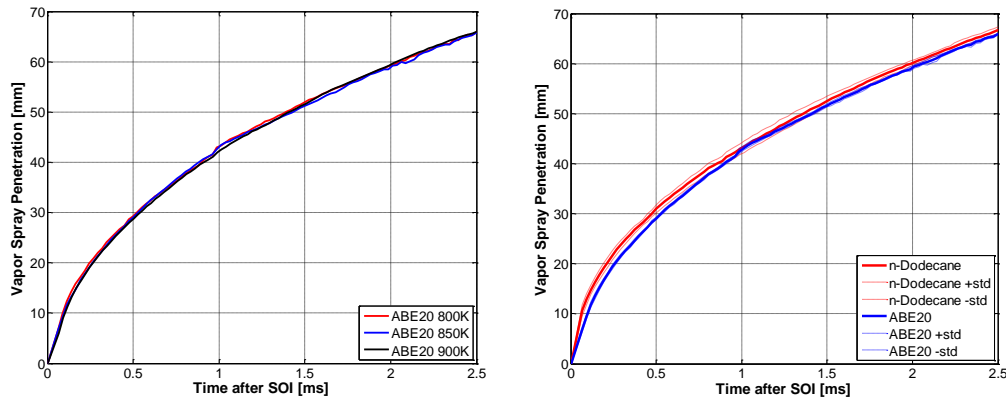

Figure 7 Vapor spray penetration length profile averaged on 12 repetitive tests.

Lift-Off Length (LOL)

The LOL is determined by the region where the flame stabilizes, and where the spray velocity and flame front velocity are balanced. A longer LOL will provide more time and space for fuel droplets to evaporate and mix with the ambient air [3]. From Figure 8 (left), it can be seen that both fuels show shorter LOL at higher ambient temperature as also found by [7], [18], because the increase in ambient temperature improves evaporation and mixing processes. LOL for ABE20 are longer than for n-dodecane for all temperatures. As mentioned previously, even though ABE20 has a faster evaporation rate, it is a blend of fuels with higher latent heat than n-dodecane, up to 250 % for ethanol. This induces a cooling effect in the chamber and an increase in the vaporization time for ABE20, and therefore a longer LOL and ID are expected.
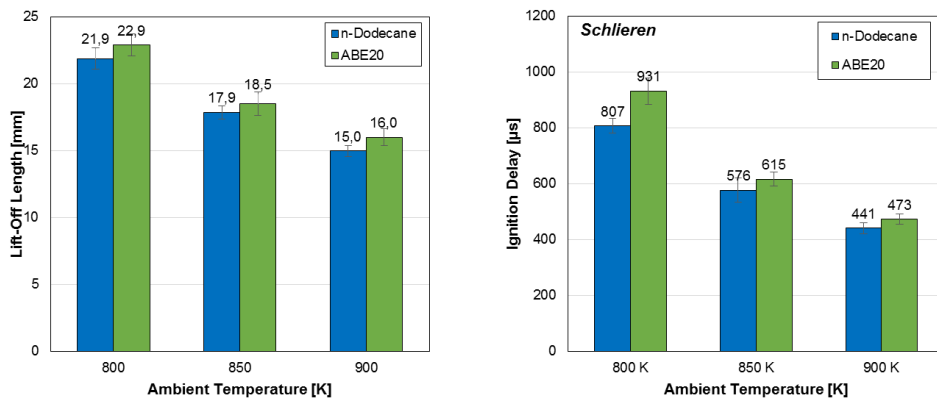

Figure 8 Lift-Off Length (left) and Ignition Delay (right) of n-dodecane and ABE20 at different ambient gas temperatures.

Ignition Delay (ID)

This part presents the results of ignition delay (ID) of the Schlieren technique, identified as the hot flame ignition delay, as shown in Figure 8 (right). As mentioned earlier, there is a relationship between LOL and ID. Both ID and LOL increase with the decrease in ambient temperature. This is due to the fact that the fuel atomization and evaporation rate at lower ambient temperature are lower than at high temperature, lowering the chemical reaction rate [7]. As expected, the higher resistance to auto-ignition of ABE20 induces a higher ID for all testing conditions,

because the ABE20 was blended with lower cetane fuels than n-dodecane (CN=74), such as ethanol (CN=8) and butanol (CN=17) [11].

Conclusions

To characterize spray and combustion parameters, the standard optical set-ups and image post-processing defined by the ECN were installed on the NOSE, a high-pressure high-temperature combustion chamber. From the experimental results presented, focusing on a comparison between ABE20 fuel and n-dodecane for 3 different ambient temperatures, it can be concluded that:

- The LL of both fuels decreases with an increase in ambient temperature due to more energy entrainment on the liquid fuel which increases the evaporation rate and reduces the surface tension and viscosity of the fuel.
- The increase in ambient temperature improves the evaporation and mixing process because of shorter lift-off length and ignition delay.
- The LL of ABE20 is shorter than that of n-dodecane due to its being blended with high volatility fuels that evaporate more easily, but ABE20 exhibits a similar trend of S compared to n-dodecane.
- The higher latent heat of vaporization in ABE20 decreases the saturation temperature, increasing the lift-off length.
- The lower auto-ignition ability of ABE20 is indicated by the lower cetane number of blended fuel in ABE20.
- The ignition delay results of the two techniques are in good agreement.

Acknowledgements

References

[1] Wu, M., Wang, M., Liu, J., and Huo, H., 2008, Biotechnology Progress, pp. 1204–1214.
[2] Nigam, P. S., and Singh, A., 2011, Progress in Energy and Combustion Science, 37 (1), pp. 52–68.
[3] Wu, H., Nithyanandan, K., Zhou, N., Lee, T. H., Lee, C. F. F., and Zhang, C., 2015, Fuel, 142, pp. 109–116.
[4] M. Tuner, 2016, SAE Technical Paper, 2016-01-0882.
[5] No, S. Y., 2016, Fuel, 183, pp. 641–658.
[6] Karimi, K., Tabatabaei, M., Horváth, I. S., and Kumar, R., 2015, Biofuel Research Journal, 8, pp. 301–308.
[7] Wu, H., Nithyanandan, K., Zhang, J., Lin, Y., Lee, T. H., and Lee, C. F., 2015, Applied Energy, 149, pp. 367–378.
[8] Chang, Y. C., Lee, W. J., Lin, S. L., and Wang, L. C., 2013, Applied Energy, 109, pp. 182–191.
[9] Engine Combustion Network, https://ecn.sandia.gov ([cit. 14-03-2017]).
[10] Nilaphai, O., Hespel, C., Moreau, B., Contino, F., Bourgeois, N., Chanchaona, S., Foucher, F., and Mounaïm-Rousselle, C., Sep. 4.-7. 2016, 27th Annual Conference on Liquid Atomization and Spray Systems.
[11] National Renewable Energy Laboratory, http://www.nrel.gov/docs/fy14osti/61693.pdf ([cit. 14-03-2017]).
[12] National Center for Biotechnology Information, https://www.nih.gov ([cit.14-03-2017]).
[13] Couch, H. T., Kozicki, W., Sage, B. H., 1963, Journal of Chemical and engineering data, 8 (3), pp. 346-349.
[14] Siebers, D. L., 1998, SAE Technical Paper, 107 (724), pp. 1205–1227.
[15] Meijer, M., Galle, J., Somers, L. M. T., Griensven, J. G., and Verhelst, S., 2013, SAE International Journal of Engines, 6 (2), pp. 1238–1248.
[16] Bardi, M., Bruneaux, G., and Malbec, L., 2016, SAE Technical Paper, 2016-01-0845.
[17] Siebers, D. L., and Higgins, B., SAE Technical Paper, 2001-01-0530.
[18] Payri, R., Salvador, F. J., Manin, J., and Viera, A., 2016, Applied Energy, 162, pp. 541–550.
[19] Dec, J. E., and Espey, C., 1998, SAE Technical Paper, 982685.
[20] Pickett, L. M., Kook, S., and Williams, T. C., 2009, SAE International Journal of Engines, 2009-01-0658.